CPC(HEP & NP), 2012, **36**(11): 1150–1156 **Chinese Physics C** Vol. 36, No. 11, Nov., 2012

Absorbed dose estimations of ^{131}I for critical organs using the GEANT4 Monte Carlo simulation code

Ziaur Rahman[1] Shakeel ur Rehman[2] Waheed Arshed[1] Nasir M Mirza[2]
Abdul Rashid[1] Jahan Zeb[1]

[1] Health Physics Division, Pakistan Institute of Nuclear Science & Technology,
Nilore, Islamabad 45650, Pakistan
[2] Department of Physics & Applied Mathematics, Pakistan Institute of Engineering &
Applied Sciences, Nilore, Islamabad 45650, Pakistan

Abstract: The aim of this study is to compare the absorbed doses of critical organs of ^{131}I using the MIRD (Medical Internal Radiation Dose) with the corresponding predictions made by GEANT4 simulations. *S*-values (mean absorbed dose rate per unit activity) and energy deposition per decay for critical organs of ^{131}I for various ages, using standard cylindrical phantom comprising water and ICRP soft-tissue material, have also been estimated. In this study the effect of volume reduction of thyroid, during radiation therapy, on the calculation of absorbed dose is also being estimated using GEANT4. Photon specific energy deposition in the other organs of the neck, due to ^{131}I decay in the thyroid organ, has also been estimated. The maximum relative difference of MIRD with the GEANT4 simulated results is 5.64% for an adult's critical organs of ^{131}I. Excellent agreement was found between the results of water and ICRP soft tissue using the cylindrical model. *S*-values are tabulated for critical organs of ^{131}I, using 1, 5, 10, 15 and 18 years (adults) individuals. *S*-values for a cylindrical thyroid of different sizes, having 3.07% relative differences of GEANT4 with Siegel & Stabin results. Comparison of the experimentally measured values at 0.5 and 1 m away from neck of the ionization chamber with GEANT4 based Monte Carlo simulations results show good agreement. This study shows that GEANT4 code is an important tool for the internal dosimetry calculations.

Key words: mean absorbed dose rate, GEANT4, Monte Carlo simulation and ^{131}I critical organs

PACS: 87.55.dk, 87.53.Bn, 87.55.K **DOI:** 10.1088/1674-1137/36/11/021

1 Introduction

Radioiodine ^{131}I is most widely used in radiotherapy for thyrotoxicosis and for the treatment of differentiated thyroid cancer, due to its appropriate value of half-life and favorable values of its beta- and gamma-ray energies. While it has been in clinical use for over 50 years, significant controversy persists regarding the types of diseases and the recommended amount of doses of radioiodine [1]. Worldwide, 2.4 time increase in the incidence rate of papillary type thyroid cancer has been observed due to radiation as the beset defined contributing factor for it [2]. A nine-fold increased risk of thyroid cancer has been observed for radiotherapy of Hodgkin's disease so strict measures need to be adopted to minimize the side-exposure of sensitive organs that are vulnerable to radiation injury [3]. To evaluate the risks and benefits of radiopharmaceuticals used for diagnostic or therapeutic purposes in nuclear medicine, reliable estimates of radiation-absorbed dose are necessary. Consequently, accurate assessment of the dose into the thyroid has gained significant importance in recent past years.

For the calculation of radiation absorbed doses into different target organs, a number of Monte Carlo codes, such as EGS [4], MCNP [5], MABDOSE [6] & GEANT4, are available. Besides that, MIRD (Medical Internal Radiation Dose) Committee of the society of nuclear medicine published several methods for calculating internal radiation doses. This scheme of dose estimation provides a logical approach towards combining biological distribution data, clearance and physical properties of radionuclides, to estimate the

---

Received 13 February 2012

internal doses [7]. Monte Carlo simulation is a highly efficient emerging tool among medical physicists working in the field of nuclear medicine, especially for simulation of routinely used devices, such as detectors, collimators & shields, and evaluating the radiation absorbed doses in diagnostic and therapeutic protocols. Recently particular interest has been shown towards the use of the Monte Carlo simulations in studying the beta and gamma emitting radionuclides used for diagnostic and therapeutic purposes [8]. The MCNP Monte Carlo simulation code has been used by Mowlavi et al. [9] to estimate the influence of thyroid volume on the energy deposition from ^{131}I. Meo et al. [8] used the GEANT4 simulation code for measuring the dose rate from ^{90}Y-labled radiopharmaceuticals to patients. Amato E et al. [10] used the GEANT4 simulation code for estimating the absorbed fraction in ellipsoidal volumes for the beta radionuclides employed in internal radiotherapy. Several image based computational codes, such as SIMDOS, RTDS, RMDP and 3D-1D, have been used in clinical situations for calculating internal doses [7]. Several authors have carried out the validation of the GEANT4 results with respect to the experimental data and to other Monte Carlo codes such as MCNP or EGS, especially for electromagnetic process and for medical applications [11].

The aim of this study is to compare the mean absorbed doses of critical organs of ^{131}I using MIRD with the corresponding predictions made by GEANT4 simulations. S-values (mean absorbed dose rate per unit activity) and energy deposition per decay for critical organs of ^{131}I for various ages, using a standard cylindrical thyroid phantom comprising water and ICRP soft-tissue material, have also been estimated. In this study the effect of the volume reduction of the thyroid, during radiation therapy, on the calculation of absorbed dose is also estimated using GEANT4. The results were compared with the already published results of Siegel & Stabin [12]. Photon specific energy deposition in the other organs of neck, due to ^{131}I decay in the thyroid organ, has also been estimated. The equivalent dose from a radioactive thyroid at the surface and at a distance of 1 m from the neck, has also been estimated using experimental measurement and the GEANT4 code.

2 Materials and methods

The MIRD Committee develops standard methods to estimate the average absorbed doses to an organ which is the sum of the products of S-values (mean absorbed dose rate per unit activity) and cumulated activity from different source organs. MIRD pamphlets have tabulated the S-values for different kinds of radioisotopes based on the specific geometry of reference patients. MIRDOSE3 [7] has been used in the nuclear medicine community since 1994 for internal radiation dosimetry. Besides normal organs, the dose of a tumor can also be estimated by usingn a nodule module in this software which utilizes the absorbed fractions for spheres of different sizes, published in MIRD Pamphlet 3 and 8.

In this study the GEANT4 code is utilized for the estimation of the results. GEANT4 is a C^{++} package which simulates a particle's interaction with matter. The physics processes available in GEANT4 cover a complete set of particles and materials over a wide range of energy. Hadronic, electromagnetic and optical processes for interactions from a few hundred eV to several hundred TeV, is accessible. In addition to physics processes, it also offers a complete set of functionality, like tracking, visualization and geometry description. A key aspect of GEANT4 is that it offers a number of independent models for utilizing similar physics processes. PENELOPE, LIVERMORE and STANDARD are the three physics models used for electron and photon transport in GEANT4. These simulation models comprise various types of interactions including photoelectric effect, Compton scattering, ionization interactions, Rayleigh scattering, fluorescence photons, and Auger electrons [13]. Due to the flexibility of GEANT4 and the accessibility of diverse physics models, the toolkit is extensively used by various experimental communities, ranging from HEP (high energy physics) accelerator physics, astrophysics, and medical physics. The accuracy of GEANT4 regarding electron and photon physics has been investigated by several groups, and detailed discrepancies among these physical models are discussed in literature [14].

The GEANT4 simulation code has been used to estimate the S-values for the critical organs of ^{131}I, for various ages. For S-values an estimation cylindrical model with principal axes at the ratio of 1/1/0.75, using water and ICRP soft tissue as material for different organs was considered. Masses of different organs and various ages are shown in Table 1, using the ICRP 53 report [15]. Comparison of the GEANT4 results about S-values for adults were made with the S-values from Pamphlet No.11 [16] published by the MIRD Committee. The same procedure has been adopted for energy deposition per decay for different ages and organs, using a cylindrical model.

Table 1. Masses (g) of critical organs of ^{131}I for different ages.

organ	1 year	5 years	10 years	15 years	adults
thyroid	1.78	3.45	7.93	12.4	20
kidneys	62.9	116	173	248	310
stomach wall	21.8	49.1	85.1	118	150
stomach contents	34.4	71.3	126	185	250
bladder wall	7.70	14.5	32.2	35.9	45
bladder contents	31.2	61.4	97.3	152	200
upper large intestine contents	27.3	55	92.5	167	220
upper large intestine wall	27.8	55.2	93.4	176	210

The GEANT4 simulation code has been used to calculate the energy deposition per decay and S-values of the beta- and gamma-rays of ^{131}I for the cylindrical thyroid model of various sizes ranging from 1–25 cm^3, using water as the thyroid material. The estimated results were compared with the published results of Siegel and Stabin. Simulations have also been performed for specific energy deposition per decay for other organs of the neck such as neck tissue, skin, and spine, with respect to the thyroid volume.

In GEANT4 simulations every organ was considered as the cylindrical volumetric source in which ^{131}I is distributed uniformly. Beta particles do not deposit their energy at the initial point, but they undergo many Coulomb interactions, so a small portion of their energy, near the surface of the organ escapes and is stored out of the source volumes. The gamma spectrum of ^{131}I has a peak energy of 0.365 MeV with 0.853 emission probability and 0.389 MeV energy per transformation while the beta spectra have an average energy of 0.183 MeV per transformation [17]. In simulations we considered the total energy per transformation.

The experimental measurements were carried out using a neck phantom (Biodex Medical System, Model: 043-365 Uptake Neck Phantom) [18]. The dose equivalent was measured with a portable survey meter (FAG Model FH 40F2) using 100–900 μCi of ^{131}I. In this regard, the dose equivalent was measured at places on the surface, 0.5 and 1 m away from the neck. The calibration of the dosimeter and its response as a function of energy were assessed in the interval between 34 and 662 keV in the Secondary Standard Dosimetry Lab (SSDL), PINSTECH.

The simulated set-up consisted of two concentric cylinders, with the inner one representing the cylindrical thyroid and the outer one representing the neck of 12.7 cm in height and 6.35 cm in radius as mentioned by Biodex Medical Systems [18]. The standard size cylindrical detector (7.62 cm in height; 3.81 cm in radius) was placed at the surface, 0.5 and 1 m distance away from the neck, for estimating the results.

For good statistical results 10^7 histories (number of particles) were generated for each measurement and each measurement was repeated three times. The simulated dose rate was calculated using the following relation [19]:

$$\dot{D}\,(\mathrm{Gy/h}) = \frac{A\,(\mathrm{Bq}) \times E\,(\mathrm{J}) \times C}{N \times M\,(\mathrm{kg})},$$

where $\dot{D}$ is the absorbed dose rate in Gy/h, E is the deposited energy in Joule (J), A is the source activity in Bq, C is the conversion factor (C=3600), N is the number of histories generated, and M is the detector mass in kg. The comparison between various parameters is presented as percentage relative difference calculated by the difference (%)=$\left[\left(\frac{E_{\mathrm{R}}-E_0}{E_0}\right)\cdot 100\right]$ where E_{R} is the reference deposited energy and E_0 corresponds to the value to be compared.

3 Results and discussions

The results for S-values for various critical cylindrical organs of adults, using MIRD and GEANT4 simulations, are given in Table 2. The table shows that good agreement is found between the two methodologies. The maximum relative difference between the MIRD and the GEANT4 simulated results is 5.64% for a cylindrical thyroid.

The first possible reason for the observed difference is the model used for simulation. The MIRD Committee utilized an ellipsoid model for organs, and in this study we use cylindrical model. The discrepancy due to the model used is very small. Ellett and Humes [20] confirm that, for small target volumes the absorbed fractions are not a very sensitive function of target shape, so it should be possible to interpolate the tabulated data for most geometries of clinical interest. The second reason is the spectrum used for the simulation, which is different from the one used for the MIRD Committee's calculation.

The MIRD spectrum is not available, so we utilize the ^{131}I spectrum as given by Cember [17]. The third reason is the backscattered photons from the surrounding tissue. Brownell et al. [21] shows that the average absorbed doses increase with backscattered photons. In this study the absorbed doses for critical organs of ^{131}I were estimated without considering the contribution of photons coming from the surrounding organs. We consider organs as an isolated volumetric source with no surrounding tissue, from which only a very small fraction of beta energy (∼1%) escapes from organs while the photon emission is more (∼96%). Another main reason is the cross section used in simulation which is different from the MIRD X-sections. GEANT4 uses the updated NIST XCOM cross section libraries. Cirrone et al. shows that the cross-sections of all the GEANT4 photon models are in statistical agreement with the NIST database [22].

Besides the comparison of the MIRD and GEANT4 schemes, two materials for these organs were also tested in this study. Comparison of the water and ICRP soft tissue used in the GEANT4 simulation for different cylindrical organs of adults is shown in Table 3. The maximum relative difference among the GEANT4 estimated results for water with ICRP soft tissue is 1.03%.

The water and ICRP soft tissue materials have the same atomic densities but different atomic compositions. It has been shown by Ellett & Humes [20] that the absorbed fraction is increasingly sensitive to atomic composition for photon energies less than 100 keV. On the basis of relative differences between these materials, it is suggested that water be used as the phantom material in place of ICRP tissue for dosimetry purposes.

S-values for the critical organs of ^{131}I, using 1, 5, 10, 15 and 18 years (adults) individuals, are shown in Table 4. Since the dose is inversely related to mass, the results show that the mean absorb doses decreases as the age of individual increases. For a specific age of individual the S-value increases as the organ mass decreases.

Table 2. S-values comparison between the GEANT4 simulations and the MIRD results.

	S-values (rad/μCi·h)		
organs	GEANT4 simulation	MIRD	relative difference(%)
thyroid	2.08E-02	2.20E-02	5.64
kidneys	1.49E-03	1.50E-03	0.78
stomach	9.22E-04	9.70E-04	4.99
bladder	1.14E-03	1.20E-03	5.08
large intestine	1.04E-03	1.10E-03	5.41

Table 3. Comparison of the water and ICRP soft tissue used in the GEANT4 simulation for different cylindrical organs of adults.

	S-values (rad/μCi·h)		
organs	water	ICRP soft tissue	relative difference (%)
thyroid	2.08E-02	2.05E-02	1.03
kidneys	1.49E-03	1.49E-03	0.05
stomach	9.22E-04	9.12E-04	1.03
bladder	1.14E-03	1.13E-03	0.92
large intestine	1.04E-03	1.03E-03	0.99

Table 4. S-values for critical organs of ^{131}I, using 1, 5, 10, 15 and 18 years (adults) individual.

	S-values (rad/μCi·h)				
organs	adults	15 years	10 years	5 years	1 years
thyroid	2.08E-02	3.30E-02	5.10E-02	1.15E-01	2.20E-01
kidneys	1.49E-03	1.86E-03	2.59E-03	3.84E-03	6.84E-03
stomach	9.22E-04	1.22E-03	1.76E-03	3.03E-03	6.04E-03
bladder	1.14E-03	1.47E-03	2.25E-03	3.50E-03	6.73E-03
large intestine	1.04E-03	1.34E-03	2.36E-03	3.86E-03	7.67E-03

Figure 1 shows the variation of the total energy deposition per decay against the critical organs of ^{131}I for individuals of different ages, using the cylindrical model. The energy deposition per decay increases for a particular age individual as the volume/mass of an organ increases because of the increasing ratio of volume to surface for a cylinder organ, causes the decrease of radiations fraction escaping from the thyroid. The same reason is valid for a particular organ of different ages, with increasing energy deposition as the age increases.

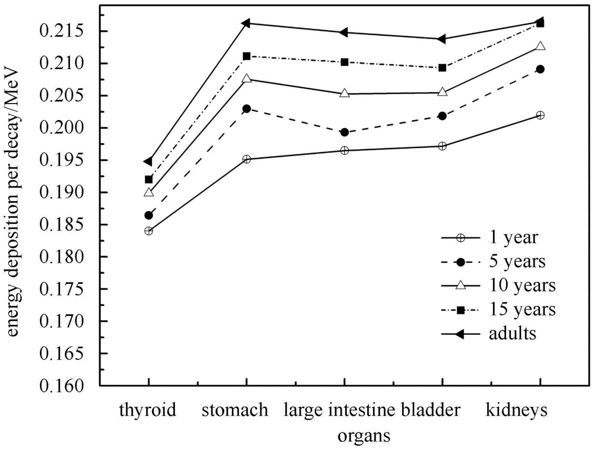

Fig. 1. Variation of the total energy deposition per decay against the critical organs of ^{131}I for different ages, using the cylindrical model.

Figure 2 shows the variation of the total energy deposition per decay of ^{131}I for both beta and gamma rays against the volume of a cylindrical shape thyroid. The total energy deposition per decay increases with volume, because the increasing ratio of volume to surface of a cylinder thyroid causes the decrease of radiation fraction escaping from the thyroid. Reported data in literature show that the thyroid volume substantially reduces (up to 70%–80%) after radioiodine therapy of Graves' hyperthyroidism is common and several authors have also recently shown that the success of this therapy depends on the absorbed dose to the thyroid. So a physician must clearly determine the volume of thyroid, so that the exact dose is delivered to a patient treated with ^{131}I [23].

Variation of S-values against the thyroid volume is shown in Fig. 3. A comparison of the GEANT4 result with Siegel and Stabin's results shows good agreement. Siegel and Stabin evaluated the absorbed fractions for electron and beta sources uniformly distributed within the spheres of various sizes using the methodology developed by Berger, with the energies varying from 0.062 to 1.428 MeV and from 0.025 to 4 MeV, respectively. The maximum relative difference between the GEANT4 cylindrical model and the Siegel & Stabin result is 3.07%.

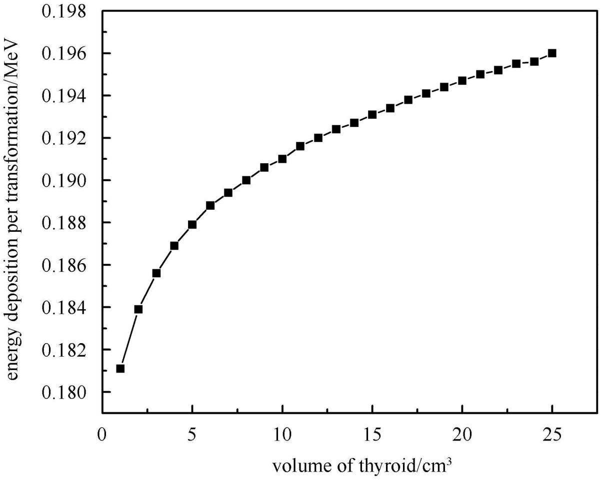

Fig. 2. Variation of the total energy deposition per decay against the volume of a thyroid for the cylindrical model.

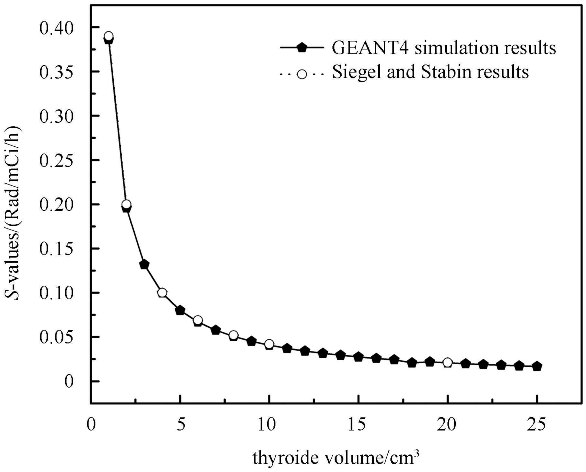

Fig. 3. S-values as a function of thyroid volume for the cylindrical model and Siegel & Stabin.

There are many reasons for this discrepancy. The first reason is the cross-section libraries used in the Berger method and the GEANT4 standard model. The second reason is the scattering contribution from the surrounding tissue. The third reason is due to the consideration of the full beta and gamma transport in our calculation. The slight difference also comes from the material, model and spectrum of ^{131}I used in our simulation, which are different from those used by Siegel and Stabin [12].

Photon specific energy deposition per decay, in the other organs of the neck, due to decay in the thyroid, has also been simulated. It is clear from Fig. 2 that the energy deposition per decay is proportional to the thyroid size. The energy deposition in other organs of the neck as a function of the thyroid volume per decay of ^{131}I is shown in Fig. 4. For neck tissue and skin the specific energy deposition is not very sensitive to the cylindrical thyroid volume but for spinal bone the specific energy deposition decreases slightly as the thyroid volume increases.

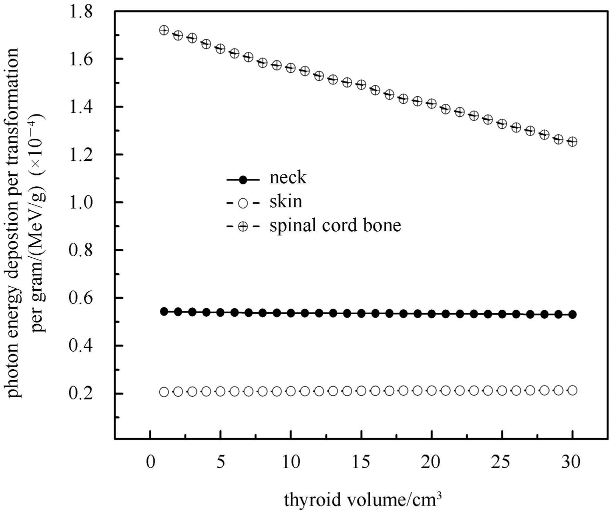

Fig. 4. Variation of specific energy deposition per decay for other organs of neck with respect to the thyroid volume.

Variation of dose rate against activity at places 0.5 and 1 m away from the cylindrical neck, using ionization detectors and GEAN4 simulation is shown in Fig. 5. The dose rate is directly related to activity and also increases with the decrease of distance. Comparison of the experimentally measured values at 0.5 and 1m away from the neck using an ionization chamber, with GEANT4 based Monte Carlo simulations results show good agreement. Although there are many factors which perturb the experimental results including the detector response, the detector position causes significant change and the location of the thyroid slot in the neck phantom.

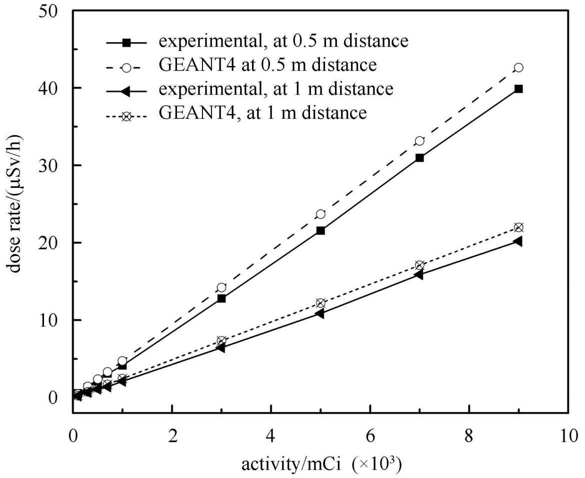

Fig. 5. Variation of dose rate against activity 0.5 and 1 m away from the cylindrical neck, using ionization detectors and GEANT4 simulation. The error bars are smaller than the box dimensions.

Comparison of the experimentally measured dose rate at the neck surface, using an ionization chamber with GEANT4 simulation results is given in Table 5. The maximum relative differences are no more than 8.38%. The difference, as explained earlier, is due to the energy response of the detectors and asymmetry found in the neck phantom.

Table 5. Comparison of dose rate at the thyroid surface with ionization chamber detectors and GEANT4 simulation.

activity/μCi	dose rate (μSv/h) at surface, experimental	dose rate (μSv/h) at surface, GEANT4	relative difference(%)
100	14.25±1.5	15.48±0.3	7.95
300	42.55±2.1	46.44±0.4	8.38
500	71.96±3.4	77.40±0.3	7.03
700	99.56±3.9	108.37±0.5	8.13
1000	142.84±4.2	154.81±0.4	7.73
3000	431.15±8.6	464.42±0.3	7.16
5000	719.34±7.9	774.04±0.5	7.07
7000	1002.65±15.9	1083.66±0.4	7.48
9000	1293.75±20.5	1393.27±0.6	7.14

4 Conclusion

This study shows that the GEANT4 code is an important tool for internal dosimetry calculations. The estimated results for cylindrical organ models show excellent agreement with the corresponding MIRD results. The simulation results reveal that without the loss of accuracy, water can be used as organ material in place of ICRP soft tissue for internal dosimetry purposes. Since the total energy deposition per decay is associated with the volume of the thyroid, physicians must clearly determine the volume of the thyroid, so that the exact dose can be delivered to a patient treated with I^{131}. Finally, it is concluded that GEANT 4 Monte Carlo simulations can be used as the standard for the comparison of experimental measurements.

References

1 Clarke SEM. Clinical Oncology, 2010, **22**: 430–437
2 Dawson P, Punwani S. European J of Radiology, 2009, **69**: 74–79
3 Green D M, Hyland A, Barcos M P et al. J Clin. Oncl., 2000, **18**(7): 1492–1497
4 Bielajew A, Rogers D. Nucl. Instrum. Methods B, 1987, **18**: 165–181
5 Briesmeister J F, ed. MCNP-A General Monte Carlo N-Particle Transport Code, Version 4C. Los Alamos National Laboratory, 2000, LA-13709-M
6 Johnson T K. Comp. Methods Programs Biomed, 1988, **27**: 159–167
7 Stabin M G, Flux G D. Biomed Imaging Interv J, 2007, **3**(2): e 28
8 Sergio Lo Meo, Gianfranco Cicoria, Giancarlo Montini et al. Nuclear Medicine Communications, 2008, **29**: 1100–1105
9 Mowlavi A A, Fornasier M R, de Denaro Mario. Radiol Oncol, 2011, **45**(2): 143–146
10 Amato E et al. Absorbed Fractions in Ellipsoidal Volumes for Beta Radionuclide's Employed in Internal Radiotherapy Phys. Med. Biol., 2009, 544171–544180
11 Amako K, Guatelli S, Ivanchencko V et al. Nucl. Physics B, 2006, **150**, 44–49
12 Siegel J A, Stabin M G. J Nucl. Med., 1994, **35**: 52–56
13 Agostinelli S, Allison J, Amako K et al. Instrum. Methods A, 2003, **506**: 250–303
14 Allison J. IEEE Trans. Nucl. Sci., 2006, **53**: 270–278
15 International Commission on Radiological Protection. Radiation Doe to Patients from Radiopharmaceutical. Publication 53. Annals of ICRP, 18, No. 1–4, Pergmon Press, 1988
16 Snyder W S, Ford M R, Warner G G, Watson S B. MIRD Pamphlet No. 11: "S" Absorb dose per Unit Cumulated Activity for Selected Radionuclide's and Organs. New York: Society of Nuclear Medicine, 1975
17 Cember H, Thomas E. Johason, Introduction to Health Physics. New York: McGraw-Hill, 2009
18 Biodex Medical Systems, 043-365 Uptake Neck Phantom Manufacturer Specifications, 2012
19 Kadri O, Gharbi F, Farah K, Mannai K, Trabelsi A, Applied Rad and Isot, 2006, **64**: 170–177
20 Ellett W H, Humes R M. J Nucl. Med., 1971, **12**(Suppl 5): 25–32
21 Brownell G L, Ellen W H, Reddy A R. The Society of Nuclear Medicine: MIRD Pamphlet 3. J Nucl. Med., 1968, **9**(suppl l): 27–39
22 Cirrone G A P, Cuttone G, Rosa F Di. Nucl. Instrum. Methods in Physics A: 2010, **618**: 315–322
23 Triono A C, di Martino F, Lazzeri M, Stabin M G. Phys. Med. Biol., 2000, **45**: 121–129